




Article

# On Catalytic Behavior of Bulk Mo<sub>2</sub>C in the Hydrodenitrogenation of Indole over a Wide Range of Conversion Thereof

Marek Lewandowski <sup>1,2,\*</sup> , Rafał Janus <sup>1,2</sup> , Mariusz Wądrzyk <sup>1,2</sup> ,  
Agnieszka Szymańska-Kolasa <sup>3</sup>, Céline Sayag <sup>4</sup> and Gérald Djéga-Mariadassou <sup>4</sup>

<sup>1</sup> Faculty of Energy and Fuels, AGH University of Science and Technology, al. A. Mickiewicza 30, 30-059 Kraków, Poland; rjanus@agh.edu.pl (R.J.); wadrzyk@agh.edu.pl (M.W.)

<sup>2</sup> AGH Centre of Energy, AGH University of Science and Technology, ul. Czarnowiejska 36, 30-054 Kraków, Poland

<sup>3</sup> Johnson Matthey plc, Emission Control Technologies, Orchard Road, Royston SG85HE, Hertfordshire, UK; Agnieszka.Szymanska-Kolasa@matthey.com

<sup>4</sup> Sorbonne Université, CNRS, Laboratoire Réactivité de Surface (LRS), 4 place Jussieu, F-75005 Paris, France; celine.sayag@sorbonne-universite.fr (C.S.); djega.gerald@orange.fr (G.D.-M.)

\* Correspondence: lewandowski@agh.edu.pl; Tel.: +48-12-617-38-90

Received: 28 October 2020; Accepted: 18 November 2020; Published: 21 November 2020



**Abstract:** The catalytic activity of bulk molybdenum carbide (Mo<sub>2</sub>C) in the hydrodenitrogenation (HDN) of indole was studied. The catalyst was synthesized using a temperature-programmed reaction of the respective oxide precursor (MoO<sub>3</sub>) with the carburizing gas mixture of 10 vol.% CH<sub>4</sub>/H<sub>2</sub>. The resultant material was characterized using X-ray diffraction, CO chemisorption, and nitrogen adsorption. The catalytic activity was studied in the HDN of indole over a wide range of conversion thereof and in the presence of a low amount of sulfur (50 ppm), which was used to simulate the processing of real petroleum intermediates. The molybdenum carbide has shown high activity under the tested operating conditions. Apparently, the bulk molybdenum carbide turned out to be selective towards the formation of aromatic products such as ethylbenzene, toluene, and benzene. The main products of HDN were ethylbenzene and ethylcyclohexane. After 99% conversion of indole HDN was reached (i.e., lack of N-containing compounds in the products was observed), the hydrogenation of ethylbenzene to ethylcyclohexane took place. Thus, the catalytic behavior of bulk molybdenum carbide for the HDN of indole is completely different compared to previously studied sulfide-based systems.

**Keywords:** molybdenum carbide; hydrodenitrogenation; indole; NO<sub>x</sub> emission; diesel fuel; ethylbenzene; ethylcyclohexane; contact time

## 1. Introduction

The petroleum industry is under constantly increasing pressure exerted by legislators in terms of improving the quality of diesel fuel towards reducing the toxicity of its exhaust emissions. In recent decades, the Environmental Protection Agency (EPA) has established several regulations targeted at the lowering of sulfur emission in diesel fuel from 50 down to 10 ppm [1–3]. Indeed, the decrease in sulfur content in diesel fuels has an additional advantage—it allows the use of the catalytic converters in the engines so that nitrogen oxide emissions may also be reduced. However, it is well known that organic compounds containing nitrogen are inhibitors of the hydrodesulfurization (HDS) process. That is why the permissible content of such N-compounds should also be reduced to a level below

60 ppm in order to make the very deep HDS process feasible (less than 10 ppm of S) and also reduce the emission of NO<sub>x</sub> during the combustion of fuel in an engine [4–6].

Nowadays, transition metal sulfides are commonly used as industrial catalysts of hydrotreating processes, mainly HDS and hydrodenitrogenation (HDN). However, recently transition metal nitrides and carbides (especially molybdenum and tungsten carbides and nitrides) have attracted increasing attention of researchers due to their promising potential as catalysts for use in commercial hydroprocessing and other reactions. For example, in addition to HDN and HDS [7–23], their activity has been extensively studied in other processes, i.e., hydrogenolysis, isomerization, aromatization, hydrogenation/dehydrogenation [24–29], hydrodechlorination [30,31], water gas shift (WGS) and steam reforming [32–35], hydrodeoxygenation (HDO) of bio-oils [36–41], methanation reaction and hydrogen production [42,43], as well as ring-opening [44].

The temperature-programmed reaction as a method of synthesis of high specific surface area bulk nitrides and carbides powders was originally reported by Volpe and Boudart [45,46]. In brief, it relies on a high-temperature reaction of relevant oxides with NH<sub>3</sub>/H<sub>2</sub> (nitridation) or CH<sub>4</sub>/H<sub>2</sub> (carburization) using a very slow heating rate. After synthesis, these materials are pyrophoric, and a passivation step is required to prevent the bulk oxidation thereof when exposed to air. A facile method used for this purpose is treatment with a 1 vol.% of O<sub>2</sub>/He mixture at room temperature (pulse method), which leads to the formation of an oxygen surface monolayer. Subsequently, these superficial oxygen atoms can react with hydrogen atoms incorporated into the bulk material during the nitridation or carburization processes. These hydrogen atoms can diffuse from the bulk to the surface, which can lead to the formation of –OH surface groups. As a result, two types of sites exist on the surface of nitrides or carbides prepared at high temperature after exposure to oxygen, i.e., metallic sites (transition metal atoms modified by C and/or N) and acidic ones (Brønsted groups) [47].

The nitrogen compounds present in diesel fuel are mainly non-basic-type compounds such as indoles and carbazoles, which account for approximately 70% of the nitrogen content in atmospheric gas oil (ca. 300 ppm), while the next 30% are basic-type compounds (namely quinolines) [48]. Therefore, many authors have used indole, even recently, as a model compound for the catalytic study on HDN over various catalytic systems [2,8,47,49–62].

The main goal of the present research was to investigate the catalytic behavior of bulk molybdenum carbide Mo<sub>2</sub>C in the reaction of hydrodenitrogenation of indole. The catalytic runs were carried out at a constant volume H<sub>2</sub>/feed ratio of 600, at a total pressure of 60 bar, and at the temperature of 613 K. The contact time varied between 0.13 and 1.07 s. It was found that the conversion of indole governs the preferential reaction pathway. Namely, low indole conversion favors the direct denitrogenation route, while in the case of high conversion, changes the reaction path towards full hydrogenation. This brings important advantages in terms of industrial purposes, i.e., by proper adjustment of the processing parameters, the consumption of hydrogen in HDN could be significantly reduced.

## 2. Results and Discussion

### 2.1. Characterization of the Catalyst

The specific surface area ( $S_g$ ) of the fresh passivated Mo<sub>2</sub>C was determined to be 33 m<sup>2</sup> g<sup>-1</sup>. The XRD patterns (Figure 1) collected for a passivated catalyst before and after HDN reaction may be assigned to the lattice planes of the hexagonal compact phase (hcp) β-Mo<sub>2</sub>C structures.

The sharp peak at  $2\theta = 36^\circ$  of a weak intensity may be assigned to the characteristic diffraction line of the residues of silicon carbide SiC (the reflection ascribed to (1 1 1) Miller index), which was used to dilute the catalyst in the catalytic bed (see Section 3.4). As seen, no alteration of the crystallographic structure of the Mo<sub>2</sub>C catalyst was observed after the test of HDN of indole. The experimental CO uptake of the fresh sample was equal to 142 μmol g<sup>-1</sup> and decreased down to 7.69 μmol g<sup>-1</sup> after the HDN reaction. This change may be due to the coking of the catalyst's surface. On the other hand, it should be noted that the catalyst was exposed to contact with air after it was removed from the reactor

for the purpose of studying the phase composition (XRD). This, in turn, could lead to passivation and a significant reduction in the number of active sites adsorbing CO. For this reason, care must be taken when analyzing the result of CO sorption for the spent catalyst. More details are provided in our former work [7].

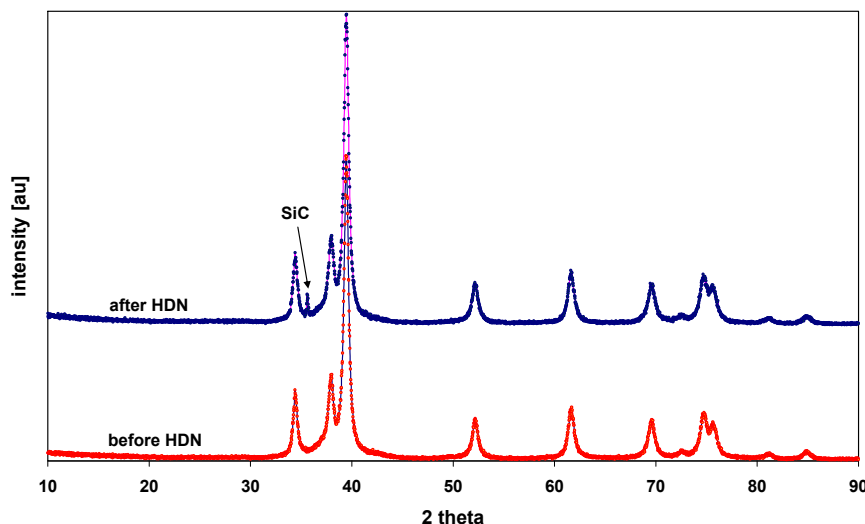
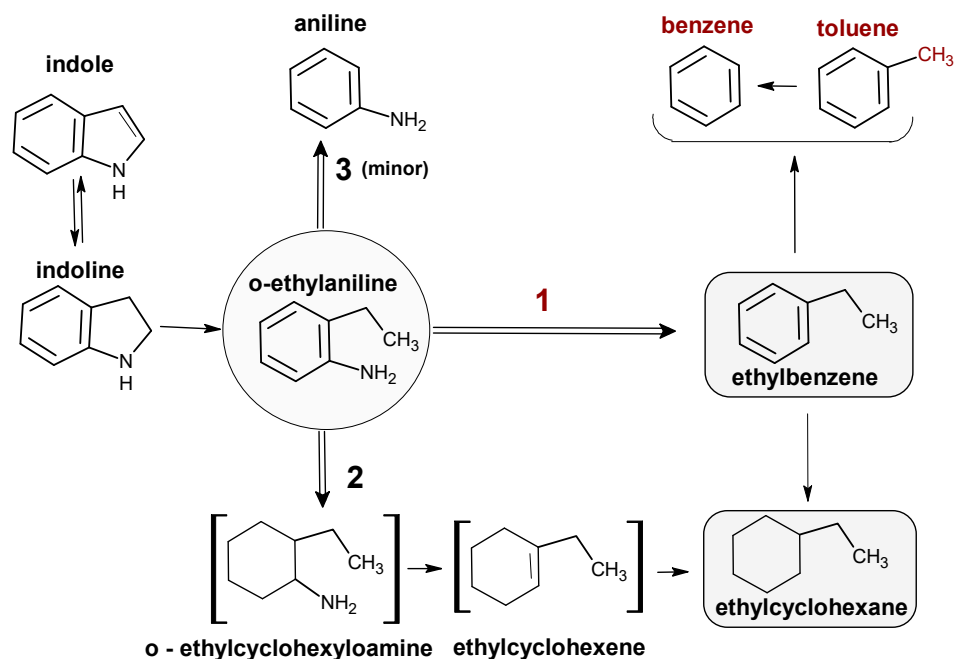


**Figure 1.** XRD patterns of molybdenum carbide ( $\text{Mo}_2\text{C}$ ) before and after hydrodenitrogenation (HDN) reaction of indole.

## 2.2. HDN of Indole over $\text{Mo}_2\text{C}$

The possible reaction scenarios of indole HDN over the bulk  $\text{Mo}_2\text{C}$  with all detected compounds are presented in Scheme 1.



**Scheme 1.** Possible reaction pathways of the hydrodenitrogenation of indole over bulk  $\text{Mo}_2\text{C}$ .

As seen, notwithstanding the further reaction pathways, the first step thereof is the hydrogenation of indole towards indoline, followed by the opening of the N-containing ring to *o*-ethylaniline (OEA).

The latter one can undergo either direct denitrogenation (called DDN route or route #1 in this work) to the ethylbenzene or full hydrogenation of the ring before denitrogenation (called HYD or route #2) to *o*-ethylaniline. The third possibility is OEA dealkylation to aniline (route #3).

It is pertinent to mention that in our research, no intermediate compound such as octahydroindole (OHI) was detected in the reaction product mixture. This is in agreement with the results presented by Bunch et al. [53] for the HDN of indole over sulfides as hydrotreating catalysts. They stated that in the presence of H<sub>2</sub>S, indole undergoes transformation to OEA because full hydrogenation of indoline into OHI was not observed. It may be concluded that in case of using molybdenum carbide, the preferred route is the formation of OEA. Benzene present in the products originates from the subsequent dealkylation of ethylbenzene (EB) and toluene (T), as well as from the hydrogenolysis of C<sub>(sp<sup>2</sup>)</sub>-N of aniline. Similar results were reported by Li et al. [8], who carried out the indole HDN process over Mo carbides and nitrides.

The presence of traces of ethylcyclohexene (EChen) for the tests with short contact time undoubtedly indicates that it was formed by the extraction of a hydrogen atom from the carbon atom in the β position of the *o*-ethylcyclohexylamine molecule (OECHA). Indeed, the hydrogenolysis of the C<sub>(sp<sup>3</sup>)</sub>-N bond of OECHA is significantly easier compared with the C<sub>(sp<sup>2</sup>)</sub>-N bond scission of OEA.

The conversion of OEA occurs following two main competitive reaction routes. The first one (route #1) results in the formation of ethylbenzene (EB), toluene (T), and benzene (B) (hydrogenolysis of C<sub>(sp<sup>2</sup>)</sub>-N bond resulting in the formation of ammonia and EB). Route #2 leads to the formation of OECHA, EChen, and ethylcyclohexane (ECH) (hydrogenation of aromatic ring to OECHA) followed by hydrogenolysis of C<sub>(sp<sup>3</sup>)</sub>-N bond resulting in the elimination of NH<sub>3</sub> and formation of ethylcyclohexene (EChen) and, ultimately, ethylcyclohexane (ECH) [47,56]. The aforementioned hydrogenolysis of C-N bond in OEA molecules occurs according to the β-elimination mechanism (Hoffman type), although it may also follow the alternative mechanism of nucleophilic substitution that would result in the same products [63]. The formation of small amounts of benzene and toluene is the result of hydrogenolysis of the C-C bond, which takes place on the metallic centers of molybdenum carbide [47].

The hydrogenation of EB towards ECH is inhibited because of the presence of nitrogen-containing compounds being stronger adsorbed on the active sites. Since measurable amounts of aniline (A) were also observed in the reaction products, an additional pathway of OEA dealkylation (route #3 in Scheme 1) could not be excluded. Aniline is formed after the hydrogenolysis of the C-C bond between the ethyl and phenyl group in the OEA molecule. However, for the sake of simplicity and taking into account the absence of OHI and the negligible amounts of aniline (<0.5%), only two pathways for the HDN of indole were considered (routes #1 and #2) as shown below and discussed hereinafter.

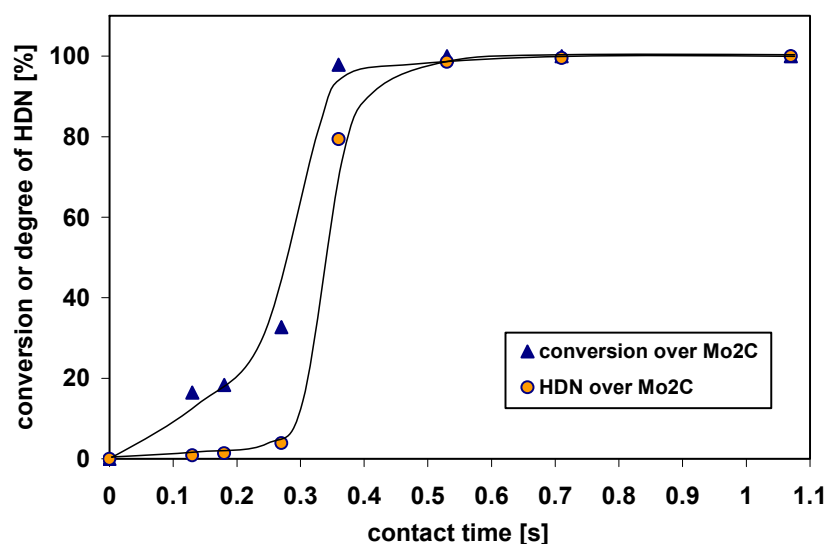
Table 1 displays the shares of indole, all the intermediates and final products, as well as total conversion, and HDN conversion over bulk Mo<sub>2</sub>C for a selected contact time of 0.37 s.

As seen, the main reaction products are ethylbenzene, ethylcyclohexane, and compounds resulting from ethylbenzene dealkylation, i.e., toluene and benzene. Moreover, nitrogen-containing compounds such as indoline, *o*-ethylaniline, and aniline were also present in the products mixture. Additionally, traces of ethylcyclohexene have been detected. The data collected in Table 1 as well as in Figure 2 indicate that molybdenum carbide shows relatively high conversion under the tested operating conditions. Indeed, for a contact time of 0.37 s, the HDN conversion (i.e., degree of HDN) over Mo<sub>2</sub>C reached 79%, while the total conversion of indole was equal to 99%.

The selectivity towards route #1 (DDN route) and #2 (HYD route) was calculated for different conversions and is presented in Table 2. Interestingly, the favored reaction pathway strongly depends on the conversion of indole (and, consequently, on contact time). Namely, in the case of low conversions (<33%), the selectivity data indicate that the HYD route (route #2) is favored, whereas for the highest conversion, the DDN route (route #1) takes over with a selectivity of 1.4 at 99% conversion. With this, it appears evident that for the highest conversion, the DDN scenario is the preferred one.

**Table 1.** Distribution of products (mole %) during the indole HDN over Mo<sub>2</sub>C catalyst at 613 K, 6 MPa, H<sub>2</sub>/feed = 600, and at a contact time of 0.37 s.

HDN Products	Share [Mole %]
<b>1—Nitrogen compounds [%]:</b>	
Indole	0
Indoline	Traces
<i>o</i> -ethylaniline (OEA)	20
Aniline (A)	Traces
<b>2—Direct denitrogenation (DDN, route #1, Scheme 1) [%]:</b>	
Ethylbenzene (EB)	34
Toluene (T)	11
Benzene (B)	2
<b>3—Hydrogenation (HYD, route #2, Scheme 1) [%]:</b>	
Ethylcyclohexane (ECH)	32
Ethylcyclohexene (ECHen)	Traces
Total conversion of indole [%] (1 + 2 + 3)	99
HDN conversion [%] (2 + 3)	79

**Figure 2.** Total conversion and degree of HDN for hydrodenitrogenation of indole over Mo<sub>2</sub>C.**Table 2.** Selectivity between route #1 and #2 for Mo<sub>2</sub>C catalyst during indole HDN carried out at 613 K, 6 MPa of H<sub>2</sub>, H<sub>2</sub>/feed = 600, S = 50 ppm.

Total Conversion over Mo <sub>2</sub> C [Mole %]	Selectivity $\frac{EB+T+B}{ECH}$
99	1.4
33	0.7
18	0.2

### 2.3. Kinetic Study of the HDN of Indole over Bulk Mo<sub>2</sub>C

Figure 3 represents the distribution of the products (as mole %) of the HDN of indole over Mo<sub>2</sub>C vs. contact times ( $t_c$ ).

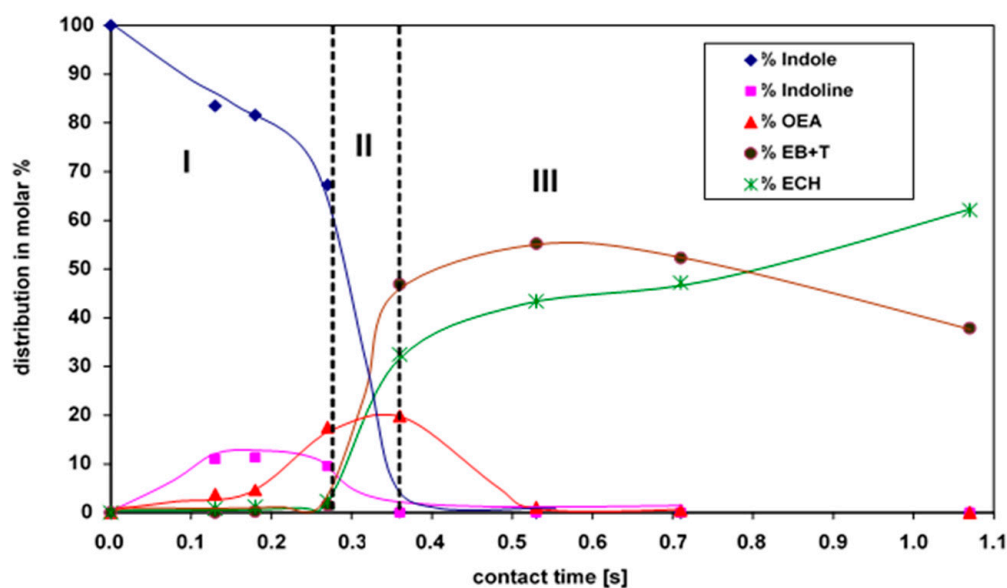


**Figure 3.** Distribution of the products of HDN of indole at different contact times in the presence of 50 ppm of sulfur over  $\text{Mo}_2\text{C}$  at 613 K, 6 MPa,  $\text{H}_2/\text{feed} = 600$ .

Apparently, three regions can be distinguished. In the first one (region I:  $t_c < 0.27$  s), the HYD route prevails with the presence of indoline and OEA to some extent. The second region (region II:  $0.27 < t_c < 0.37$  s) is characterized by a sudden decrease in indole mole fraction along with the increase in OEA mole fraction as well as a significant increase in EB and ECH concentrations. The linear drop in indole content in regions I and II indicates that the indole extinction process is of zero order. In the second region, the real HDN reaction of OEA occurred (in this region, OEA is clearly the most abundant intermediate).

When the contact time is longer than 0.37 s (region III), indole is consumed almost quantitatively (i.e., the total conversion reaches 99%). The mole fraction of OEA decreases and takes over the role of reactants leading to HDN products such as EB and ECH (Figure 3). The simultaneous increase in both EB and ECH shares indicates that the reaction occurs according to both pathways (route #1 and #2); however, it is worth noting that route #1 is the favored one. These results are contradict the results reported by Ozkan et al. [54]. Therein, the authors have shown that the presence of  $\text{H}_2\text{S}$  could invert the selectivity towards route #2. In our work, the presence of sulfur (dimethyl disulfide (DMDS) as a source of  $\text{H}_2\text{S}$ ), did not *switch* the reaction pathway. The alteration in selectivity between ECH and EB observed for  $t_c > 0.8$  s (Figure 3) is only due to the progressive hydrogenation of EB to ECH, which can occur without appreciable limitations because of the absence of N-containing compounds as shown elsewhere [57,64–70]. To the best of our knowledge, such specific behavior (i.e., the privileged pathway of aromatics formation) is a unique feature of the molybdenum carbide catalyst.

Over  $\text{Mo}_2\text{C}$ , aromatic products are favored because the nucleophilic substitution  $\text{S}_{\text{N}2}$  is the dominant mechanism governing the HDN reactions [65]. On the other hand, it is well known that the presence of indole and indoline strongly inhibits the conversion of ethylaniline [66] and, as a consequence, it inhibits the whole HDN process [67]. The formation of ethylbenzene as the dominant HDN product of indole was also reported by Piskorz et al. [68]. Based on the density functional theory (DFT) simulations, they found out that the selectivity of the reaction depends on the manner of the H: attack on the aromatic ring or the amino group of the OEA intermediate. The difference in the energy barriers between the DDN and HYD molecular paths calculated by the authors was equal to  $33.5 \text{ kJ mol}^{-1}$  ( $8 \text{ kcal mol}^{-1}$ ) [68]. This justifies the higher amounts of the aromatic compounds (i.e., EB) compared to aliphatic ones (such as ECH).

At 99% indole conversion, the dominating products are EB and ECH. When the contact time is longer than 0.54 s, there are no more nitrogen-containing products. Interestingly, a change can be seen in the preferred route of the reaction—ECH is produced with increased efficiency, while the amount of formed EB decreases. While a significant number of nitrogen-compounds are still present in the feed, hydrogenation of the unsaturated products is inhibited.

In the case of the contact time  $t_c > 0.53$  s (no N-containing compounds), the effect of the total change in the selectivity was observed. This may be associated with the hydrogenation of EB to ECH. This is in accordance with the results reported formerly by Mordenti [69], who indicated that OEA (as the main N-containing intermediate product comprising nitrogen) is responsible for blocking the catalytic centers. Consequently, the hydrogenation of ethylbenzene to ethylcyclohexane is impeded. Similar research has been published previously by Sayag [70], who presented in his work evidence supporting the proposed inhibitory effect of *o*-propylaniline (OPA) in isopropyl benzene hydrogenation to propylcyclohexane.

The same researcher with co-workers [57] studied the HDN of indole over Mo<sub>2</sub>C supported on activated carbon black composites (Mo<sub>2</sub>C/CBC). They reported a maximum HDN conversion (100%) reached over all the studied catalysts notwithstanding the contact time. The authors found out that the increase in saturated products comes only from the hydrogenation of the unsaturated ones. Indeed, while N-compounds are still present in the feed in abundant amounts, hydrogenation of the unsaturated products is inhibited because of a competitive strong adsorption of these molecules onto the Mo<sub>2</sub>C surface [57,67].

A similar phenomenon was observed by Da Costa et al. [64], who studied the influence of 4,6-dimethyldibenzothiophene (4,6-DMDBT) on hydrogenation of biphenyl (BPh) over Mo<sub>2</sub>C supported on Al<sub>2</sub>O<sub>3</sub>. When 4,6-DMDBT was present in the reaction system, the route of hydrogenation of BPh to cyclohexylbenzene (CHB) was impeded because of strong adsorption of S-compounds on the surface of the catalyst. Furthermore, a similar effect was observed in the case of HDS of dibenzothiophene (DBT) [16]; the CHB was produced from tetrahydrodibenzothiophene because of the strong adsorption of S-compounds. Furthermore, Mamede et al. [71] have observed a similar behavior when carrying out the tests of hydrogenation of toluene over Mo<sub>2</sub>C in the presence of thiophene.

For the sake of comparison, Table 3 reports the chosen literature data on HDN of indole over carbides and sulfides. Sulfide catalysts feature a high selectivity towards the saturated product (ECH), in opposition to observation over molybdenum carbide. This effect is due to the enhancement of the C<sub>(sp<sup>3</sup>)</sub>-N bond cleavage in the presence of sulfur [72] instead of the C<sub>(sp<sup>2</sup>)</sub>-N bond cleavage. The selectivity of HDN of indole over Mo<sub>2</sub>C found in majority of works is shifted towards the aromatic product (i.e., EB). This is consistent with our results (see last line in Table 3). It can be concluded that, despite the presence of 50 ppm of S, the behavior of Mo<sub>2</sub>C is completely different than that of the sulfide catalysts. The undoubted advantage of Mo<sub>2</sub>C is the possibility of significant reduction in hydrogen consumption for the process. As such, bulk Mo<sub>2</sub>C may be a promising alternative for commercial HDN catalysts used on a technological scale.

**Table 3.** Selectivity between route #1 and #2 over different catalysts tested in HDN of indole. Data from literature compared with the results reported herein.

Catalyst/Test Conditions	Temperature of Reaction [K]	Pressure [bar]	Selectivity ECH/EB	Reactor	Sulfidation Conditions	Ref.
CoMoS/Al <sub>2</sub> O <sub>3</sub>	593	50	300	Autoclave	–	[67]
NiMoS/Al <sub>2</sub> O <sub>3</sub>	593	70	15	Fixed-bed reactor	673 K; 10% H <sub>2</sub> S; 10 h	[53]
NiMoS/Al <sub>2</sub> O <sub>3</sub>	593	70	25	Fixed-bed reactor	673 K; 10% H <sub>2</sub> S; 10 h	[53]

Table 3. Cont.

Catalyst/Test Conditions	Temperature of Reaction [K]	Pressure [bar]	Selectivity ECH/EB	Reactor	Sulfidation Conditions	Ref.
NiMoS/Al <sub>2</sub> O <sub>3</sub>	593	70	40	Fixed-bed reactor	673 K; 10% H <sub>2</sub> S; 10 h	[53]
NiMoS CoMoS	613	35	7.5	Fixed-bed reactor	673 K; 10% H <sub>2</sub> S; 2 h	[73]
Mo <sub>2</sub> C/CBC no sulfur H <sub>2</sub> /feed = 600	623	50	1.25	Fixed-bed reactor	–	[74]
Mo <sub>2</sub> C/CBC H <sub>2</sub> /feed = 200	623	50	2	Fixed-bed reactor	–	[74]
Mo <sub>2</sub> C/C in situ	613	50	2	Fixed-bed reactor	–	[69,75]
Bulk Mo <sub>2</sub> C with 50 ppm of S	613	60	0.7	Fixed-bed reactor	–	This paper

### 3. Materials and Methods

#### 3.1. Materials

MoO<sub>3</sub> (≥99.5%, Honeywell Fluka™, Charlotte, NC, USA) was used as the precursor for the catalyst synthesis. The gases used were: hydrogen (H<sub>2</sub>, Air Liquide, grade C, purity > 99.995%), helium (He, Air Liquide, grade C, purity > 99.995%), argon (Ar, Air Liquide, grade C, purity > 99.995%), methane (CH<sub>4</sub>, Air Liquide, grade N30, purity > 99.9%), and oxygen (O<sub>2</sub>, Air Liquide, grade C, purity > 99.5%). Indole (>99%, Honeywell Fluka™, Charlotte, NC, USA) was used as model compound for the kinetic study. Dimethyl disulfide (DMDS, ≥98%, Honeywell Fluka™, Charlotte, NC, USA) dissolved in decaline (≥98%, Honeywell Fluka™, Charlotte, NC, USA) was used as a sulfur source.

#### 3.2. Synthesis of Bulk Mo<sub>2</sub>C

Molybdenum carbide (Mo<sub>2</sub>C) was prepared using a modified procedure reported by Volpe and Boudart [46]. The temperature profile used for the synthesis is presented in Figure 4.

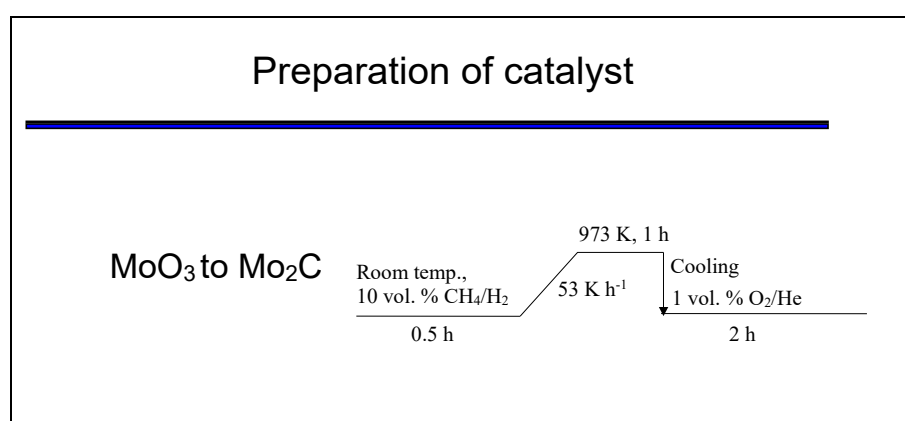


**Figure 4.** Temperature-programmed reduction (TPR) profile for the synthesis of the bulk molybdenum carbide catalyst.

Molybdenum trioxide was put on a sintered holder placed in a quartz reactor and was subjected to carburization with a mixture of 10 vol.% CH<sub>4</sub>/H<sub>2</sub> at a flow rate of 13.2 L g<sup>-1</sup> h<sup>-1</sup>. The temperature was raised linearly from 300 to 973 K at a heating rate of 53 K h<sup>-1</sup> and then the material was held



at 973 K for the next 1 h. Eventually, the sample was cooled to room temperature (RT) under the constant flow of the carburizing mixture. In the case when exposure to air was needed, the sample was passivated using 1 vol.% O<sub>2</sub>/He (pulse method) in order to form a protective oxide layer on its surface.

### 3.3. Characterization Techniques

Structural characterization of the Mo<sub>2</sub>C catalyst was carried out by means of X-ray diffraction (XRD) using a SIEMENS D-500 diffractometer (Siemens, Berlin, Germany) working with the CuK $\alpha$  monochromatized radiation ( $\lambda = 1.54184 \text{ \AA}$ ). The XRD patterns were analyzed using HighScore (Malvern Panalytical, United Kingdom) software. The degrees of crystallinity of the catalyst were estimated based on the intensity of the reflections recorded in the angular range of  $2\theta = 10\text{--}90^\circ$ .

A Quantachrome–Quantasorb Jr apparatus (Quantachrome Instruments, Boynton Beach, FL, USA) was employed for the  $S_g$  measurement in dynamic conditions. The  $S_g$  of the catalyst was calculated from the N<sub>2</sub> adsorption/desorption at different partial pressures of nitrogen. The standard  $S_g$  measurement using the Brunauer-Emmett-Teller (BET) model is based on a three-point analysis based on the adsorption of mixtures containing 10, 20, and 30 vol.% of N<sub>2</sub> in He. Prior to the measurement, the material (100 mg) was outgassed under flowing nitrogen at 623 K for 2 h.

CO adsorption is a classic technique commonly used for estimating the number of surface metallic sites. It is also employed to titrate the active centers on the surfaces of the transition metal carbides or nitrides [47,60–62]. The CO titration was performed in situ, i.e., in the synthesis reactor without exposing the fresh material to air or to the passivating mixture after synthesis. The pulses of given quantities of CO (17  $\mu\text{mol}$ ) were injected to the reactor containing Mo<sub>2</sub>C with regular intervals at RT under He flow (40 mL min<sup>-1</sup>) purified before by an oxygen trap (Oxisorb, Messer Griesheim GmbH, Bad Soden am Taunus, Germany). After each pulse, the number of CO molecules not chemisorbed was analyzed using a conventional detection system equipped with a TCD. The CO injections were continued until the probe molecule quantitatively saturated the catalyst's surface. The acquired data were processed and the number of micromoles of the chemisorbed CO per gram of the sample was calculated.

### 3.4. Kinetic Study of HDN of Indole

The HDN tests of indole were carried out using a downflow fixed-bed microreactor working in a high-pressure flow system. The catalytic tests were performed over 0.8 g of catalyst (diluted with SiC at a mass ratio SiC/Mo<sub>2</sub>C = 5:1) in the presence of sulfur (50 ppm S), evolved by the decomposition of 70 ppm dimethyl disulfide (DMDS) in the feed. The addition of sulfur was employed in order to simulate the HDN process of real petroleum intermediates that always contain certain amounts of S-compounds. The liquid feed containing 2.5 wt. % of indole dissolved in decaline was supplied to the flow manifold by a high-pressure piston pump (Gilson model 307, Artisan Technology Group, Mercury DriveIL, Champaign, IL, USA). Hydrogen flow was controlled by a mass flow controller (Brooks 5850TR, Brooks Instruments, PA, USA), while the total pressure was adjusted by a back-pressure regulator (Brooks 5866, Brooks 5850TR, Brooks Instruments, PA, USA). The temperature in the reactor oven was adjusted using a temperature controller (Hanyoung MX9, Hanyoung, Vietnam).

The kinetic study of the HDN process was performed at a total pressure of 60 bar, and a temperature of 613 K using the H<sub>2</sub>/feed volume ratio of 600 and contact times ( $t_c$ ) between 0.13 and 1.07 s. The contact time ( $t_c$ ) was calculated as follows:

$$t_c[\text{s}] = \frac{\text{Catalyst volume (cm}^3\text{)}}{\text{H}_2/\text{feed flow (cm}^3\text{ s}^{-1}\text{)}} \quad (1)$$

The liquid products were collected with constant intervals of 1 h and analyzed via manual injections (0.8  $\mu\text{L}$ ) to a gas chromatograph (HP 4890, Agilent Technologies, Santa Clara, CA, USA) equipped with a capillary column (DB1: 30 m  $\times$  0.25 mm  $\times$  0.25  $\mu\text{m}$ , Agilent Technologies, Santa Clara,

CA, USA) and a FID detector. The temperature of the injector was kept at 523 K, and the split ratio was 1:50. High-purity argon was used as the carrier gas. The oven temperature program was the following: the temperature was increased from 323 K to 453 K at a rate of 5 K min<sup>-1</sup>, and then held at 453 K for 1 min. Next, the temperature was increased from 453 K to 493 K at 10 K min<sup>-1</sup> and held at this temperature for 2 min. The total time of the analysis was 33 min.

The carbide catalyst was stabilized in situ for 10 h using a mixture of 70 ppm of DMDS solution in decaline in hydrogen (60 mL min<sup>-1</sup>) as a carrier gas, at the processing temperature under the total pressure of 60 bar.

The total conversion of indole, degree of HDN, and selectivity were calculated according to Equations (2)–(4):

$$\text{Conv. of indole [\%]} = \frac{N_N}{N_N + N_{\text{indole}}} \cdot 100\%; \quad (2)$$

$$\text{Degree of HDN [\%]} = \frac{N_H}{N_N + N_{\text{indole}}} \cdot 100\%; \quad (3)$$

$$\text{Selectivity [-]} = \frac{EB + T + B}{ECH}; \quad (4)$$

where:

$N_N$  is the mole % of all products of decomposition of indole (including N-containing compounds except indole);

$N_{\text{indole}}$  is the mole % of indole in the liquid product after reaction;

$N_H$  is the mole % of non-nitrogen products from the decomposition of indole;

EB + T + B are mole % of ethylbenzene, toluene, and benzene, respectively;

ECH means mole % of ethylcyclohexane.

#### 4. Conclusions

Molybdenum carbide was found to be active in HDN of indole in the presence of a low amount of sulfur (50 ppm). It was found that the preferred HDN reaction path depends on the indole conversion. Namely, in the case of low conversion, direct denitrogenation is the favored reaction route with EB being the main product. Contrarily, in the case of the highest conversion, the privileged pathway is the full hydrogenation towards ethylcyclohexane. The preferential direct denitrogenation route is opposite to the mechanism, which was hitherto observed over sulfide catalyst, which in general leads mainly to the hydrogenated products. Thus, the indole HDN mechanism over the bulk molybdenum carbide is different compared to that of sulfide catalysts. Over the studied Mo<sub>2</sub>C material, the hydrogenated products (such as ECH) become the main products only in the case where N-containing products are eradicated from the reactant mixture. Simultaneously, a minor dealkylation route towards aniline was observed. This brings certain significant advantages, i.e., the consumption of hydrogen in HDN processes may be significantly reduced. To the best of our knowledge, herein we report on this peculiar behavior of the Mo<sub>2</sub>C catalyst for the first time.

**Author Contributions:** Conceptualization, methodology, and investigation, M.L.; formal analysis, A.S.-K. and C.S.; writing—original draft preparation, M.L.; writing—review and editing, R.J. and M.W.; supervision and review, G.D.-M. All authors have read and agreed to the published version of the manuscript.

**Funding:** This research received no external funding.

**Acknowledgments:** The research was financed by the research subsidy of AGH University of Science and Technology, number 16.16.210.476.

**Conflicts of Interest:** The authors declare no conflict of interest.

## References

1. Wang, X.; Clark, P.; Oyama, S.T. Synthesis, characterization, and hydrotreating activity of several iron group transition metal phosphides. *J. Catal.* **2002**, *208*, 321–331. [[CrossRef](#)]
2. Breyse, M.; Djéga-Mariadassou, G.; Pessayre, S.; Geantet, C.; Vrinat, M.; Perot, G.; Lemaire, M. Deep desulfurization: Reactions, catalysts and technological challenges. *Catal. Today* **2003**, *84*, 129–138. [[CrossRef](#)]
3. Ishihara, A.; Dumeignil, F.; Lee, J.; Mitsunashi, K.; Qian, E.W.; Kabe, T. Hydrodesulfurization of sulfur-containing polyaromatic compounds in light gas oil using noble metal catalysts. *Appl. Catal. A* **2005**, *289*, 163–173. [[CrossRef](#)]
4. Sano, Y.; Choi, K.-H.; Korai, Y.; Mochida, I. Effects of nitrogen and refractory sulfur species removal on the deep HDS of gas oil. *Appl. Catal. B* **2004**, *53*, 169–174. [[CrossRef](#)]
5. Sano, Y.; Choi, K.-H.; Korai, Y.; Mochida, I. Adsorptive removal of sulfur and nitrogen species from a straight run gas oil over activated carbons for its deep hydrodesulfurization. *Appl. Catal. B* **2004**, *49*, 219–225. [[CrossRef](#)]
6. Rana, M.S.; Al-Barood, A.; Brouesli, R.; Al-Hendi, A.W.; Mustafa, N. Effect of organic nitrogen compounds on deep hydrodesulfurization of middle distillate. *Fuel Proc. Technol.* **2018**, *177*, 170–178. [[CrossRef](#)]
7. Szymańska-Kolasa, A.; Lewandowski, M.; Sayag, C.; Brodzki, D.; Djéga-Mariadassou, G. Comparison between tungsten carbide and molybdenum carbide for the hydrodenitrogenation of carbazole. *Catal. Today* **2007**, *119*, 35–38. [[CrossRef](#)]
8. Li, S.; Lee, J.S.; Hyeon, T.; Suslick, K. Catalytic hydrodenitrogenation of indole over molybdenum nitride and carbides with different structures. *Appl. Catal. A* **1999**, *184*, 1–9. [[CrossRef](#)]
9. Dhandapani, B.; Clair, T.S.; Oyama, S.T. Simultaneous hydrodesulfurization, hydrodeoxygenation, and hydrogenation with molybdenum carbide. *Appl. Catal. A* **1998**, *168*, 219–228. [[CrossRef](#)]
10. Nagai, M.; Goto, Y.; Irisawa, A.; Omi, S. Catalytic activity and surface properties of nitrated molybdena-alumina for carbazole hydrodenitrogenation. *J. Catal.* **2000**, *191*, 128–137. [[CrossRef](#)]
11. Schwartz, V.; Oyama, S.T. Reaction network of pyridine hydrodenitrogenation over carbide and sulfide catalysts. *J. Mol. Catal. A Chem.* **2000**, *163*, 269–282. [[CrossRef](#)]
12. Szymańska, A.; Lewandowski, M.; Sayag, C.; Djéga-Mariadassou, G. Kinetic study of the hydrodenitrogenation of carbazole over bulk molybdenum carbide. *J. Catal.* **2003**, *218*, 24–31. [[CrossRef](#)]
13. Da Costa, P.; Potvin, C.; Manoli, J.-M.; Breyse, B.; Djéga-Mariadassou, G. Supported molybdenum carbides lie between metallic and sulfided catalysts for deep HDS. *Catal. Lett.* **2003**, *86*, 133–138. [[CrossRef](#)]
14. McCrea, K.R.; Logan, J.W.; Tarbuck, T.L.; Heiser, J.L.; Bussell, M.E. Thiophene hydrodesulfurization over alumina-supported molybdenum carbide and nitride catalysts: Effect of Mo loading and phase. *J. Catal.* **1997**, *171*, 255–267. [[CrossRef](#)]
15. Hynaux, A.; Sayag, C.; Suppan, S.; Trawczyński, J.; Lewandowski, M.; Szymańska-Kolasa, A.; Djéga-Mariadassou, G. Kinetic study of the deep hydrodesulfurization of dibenzothiophene over molybdenum carbide supported on a carbon black composite: Existence of two types of active sites. *Catal. Today* **2007**, *119*, 3–6. [[CrossRef](#)]
16. Szymańska-Kolasa, A.; Lewandowski, M.; Sayag, C.; Djéga-Mariadassou, G. Comparison of molybdenum carbide and tungsten carbide for the hydrodesulfurization of dibenzothiophene. *Catal. Today* **2007**, *119*, 7–12. [[CrossRef](#)]
17. Lewandowski, M.; Szymańska-Kolasa, A.; Da Costa, P.; Sayag, C. Catalytic performances of platinum doped molybdenum carbide for simultaneous hydrodenitrogenation and hydrodesulfurization. *Catal. Today* **2007**, *119*, 31–34. [[CrossRef](#)]
18. Diaz, B.; Sawhill, S.J.; Bale, D.H.; Main, R.; Phillips, D.C.; Korlann, S.; Self, R.; Bussell, M.E. Hydrodesulfurization over supported monometallic, bimetallic and promoted carbide and nitride catalysts. *Catal. Today* **2003**, *86*, 191–209. [[CrossRef](#)]
19. Manoli, J.-M.; Da Costa, P.; Brun, M.; Vrinat, M.; Mauge, F.; Potvin, C. Hydrodesulfurization of 4,6-dimethyldibenzothiophene over promoted (Ni,P) alumina-supported molybdenum carbide catalysts: Activity and characterization of active sites. *J. Catal.* **2004**, *221*, 365–377. [[CrossRef](#)]
20. Al-Megren, H.A.; González-Cortés, S.L.; Xiao, T.; Green, M.L.H. A comparative study of the catalytic performance of Co-Mo and Co(Ni)-W carbide catalysts in the hydrodenitrogenation (HDN) reaction of pyridine. *Appl. Catal. A* **2007**, *329*, 36–45. [[CrossRef](#)]

21. Wang, H.; Liu, S.; Govindarajan, R.; Smith, K.J. Preparation of Ni-Mo<sub>2</sub>C/carbon catalysts and their stability in the HDS of dibenzothiophene. *Appl. Catal. A* **2017**, *539*, 114–127. [[CrossRef](#)]
22. Nagai, M.; Tung, N.T.; Adachi, Y.; Kobayashi, K. New approach to active sites analysis of molybdenum-containing catalysts for hydrodesulfurization and hydrodenitrogenation based on inverse problem, fractal and site-type analyses. *Catal. Today* **2016**, *271*, 91–101. [[CrossRef](#)]
23. Lewandowski, M.; Szymańska-Kolasa, A.; Sayag, C.; Beaunier, P.; Djéga-Mariadassou, G. Atomic level characterization and sulfur resistance of unsupported W<sub>2</sub>C during dibenzothiophene hydrodesulfurization. Classical kinetics simulation of the reaction. *Appl. Catal. B* **2014**, *144*, 750–759. [[CrossRef](#)]
24. Neylon, M.K.; Choi, S.; Kwon, H.; Curry, K.E.; Thompson, L.T. Catalytic properties of early transition metal nitrides and carbides: N-butane hydrogenolysis, dehydrogenation and isomerization. *Appl. Catal. A* **1999**, *183*, 253–263. [[CrossRef](#)]
25. Rocha, A.S.; Rocha, A.B.; Teixeira da Silva, V. Benzene adsorption on Mo<sub>2</sub>C: A theoretical and experimental study. *Appl. Catal. A* **2010**, *379*, 54–60. [[CrossRef](#)]
26. Monjardin, E.; Cruz-Reyes, J.; Del Valle-Granados, M.; Flores-Aquino, E.; Avalos-Borja, M.; Fuentes-Moyado, S. Synthesis, characterization and catalytic activity in the hydrogenation of cyclohexene with molybdenum carbide. *Catal. Lett.* **2008**, *120*, 137–142. [[CrossRef](#)]
27. Tominaga, H.; Aoki, Y.; Nagai, M. Hydrogenation of CO on molybdenum and cobalt molybdenum carbides. *Appl. Catal. A* **2012**, *423–424*, 192–204. [[CrossRef](#)]
28. Mehdad, A.; Jentoft, R.E.; Jentoft, F.C. Passivation agents and conditions for Mo<sub>2</sub>C and W<sub>2</sub>C: Effect on catalytic activity for toluene hydrogenation. *J. Catal.* **2017**, *347*, 89–101. [[CrossRef](#)]
29. Lewandowski, M.; Szymańska-Kolasa, A.; Sayag, C.; Djéga-Mariadassou, G. Activity of molybdenum and tungsten oxycarbides in hydrodenitrogenation of carbazole leading to isomerization secondary reaction of bicyclohexyl. Results using bicyclohexyl as feedstock. *Appl. Catal. B* **2020**, *261*, 118239. [[CrossRef](#)]
30. Delannoy, L.; Giraudon, J.-M.; Granger, P.; Leclercq, L.; Leclercq, G. Group VI transition metal carbides as alternatives in the hydrodechlorination of chlorofluorocarbons. *Catal. Today* **2000**, *59*, 231–240. [[CrossRef](#)]
31. Jujjuri, S.; Cárdenas-Lizana, F.; Keane, M.A. Synthesis of group VI carbides and nitrides: Application in catalytic hydrodechlorination. *J. Mater. Sci.* **2014**, *49*, 5406–5417. [[CrossRef](#)]
32. Nagai, M.; Matsuda, K. Low-temperature water–gas shift reaction over cobalt–molybdenum carbide catalyst. *J. Catal.* **2006**, *238*, 489–496. [[CrossRef](#)]
33. Barthos, R.; Solymosi, F. Hydrogen production in the decomposition and steam reforming of methanol on Mo<sub>2</sub>C/carbon catalysts. *J. Catal.* **2007**, *249*, 289–299. [[CrossRef](#)]
34. Lausche, A.C.; Schaidle, J.A.; Thompson, L.T. Understanding the effects of sulfur on Mo<sub>2</sub>C and Pt/Mo<sub>2</sub>C catalysts: Methanol steam reforming. *Appl. Catal. A* **2011**, *401*, 29–36. [[CrossRef](#)]
35. Sabnis, K.D.; Cui, Y.; Akatay, M.C.; Shekhar, M.; Lee, W.-S.; Miller, J.T.; Delgass, W.N.; Ribeiro, F.H. Water–gas shift catalysis over transition metals supported on molybdenum carbide. *J. Catal.* **2015**, *331*, 162–171. [[CrossRef](#)]
36. Sousa, L.A.; Zotin, J.L.; Teixeira da Silva, V. Hydrotreatment of sunflower oil using supported molybdenum carbide. *Appl. Catal. A* **2012**, *449*, 105–111. [[CrossRef](#)]
37. Patel, M.A.; Baldanza, M.A.S.; Teixeira da Silva, V.; Bridgwater, A.V. In situ catalytic upgrading of bio-oil using supported molybdenum carbide. *Appl. Catal. A* **2013**, *458*, 48–54. [[CrossRef](#)]
38. Chen, C.-J.; Lee, W.-S.; Bhan, A. Mo<sub>2</sub>C catalyzed vapor phase hydrodeoxygenation of lignin-derived phenolic compound mixtures to aromatics under ambient pressure. *Appl. Catal. A* **2016**, *510*, 42–48. [[CrossRef](#)]
39. Rocha, A.S.; Souza, L.A.; Oliveira, R.R.; Rocha, A.B.; Teixeira da Silva, V. Hydrodeoxygenation of acrylic acid using Mo<sub>2</sub>C/Al<sub>2</sub>O<sub>3</sub>. *Appl. Catal. A* **2017**, *531*, 69–78. [[CrossRef](#)]
40. Wang, H.; Liu, S.; Smith, K.J. Synthesis and hydrodeoxygenation activity of carbon supported molybdenum carbide and oxycarbide catalysts. *Energy Fuels* **2016**, *30*, 6039–6049. [[CrossRef](#)]
41. Machado, M.A.; He, S.; Davies, T.E.; Seshan, K.; Teixeira da Silva, V. Renewable fuel production from hydrolysis of residual biomass using molybdenum carbide-based catalysts. *Catal. Today* **2018**, *302*, 161–168. [[CrossRef](#)]
42. Huo, X.; Wang, Z.; Huang, J.; Zhang, R.; Fang, Y. Bulk Mo and Co–Mo carbides as catalysts for methanation. *Catal. Commun.* **2016**, *79*, 39–44. [[CrossRef](#)]
43. Ma, Y.; Guan, G.; Hao, X.; Cao, J.; Abudula, A. Molybdenum carbide as alternative catalyst for hydrogen production—A review. *Renew. Sustain. Energy Rev.* **2017**, *75*, 1101–1129. [[CrossRef](#)]

44. Ardakani, S.J.; Liu, X.; Smith, K.J. Hydrogenation and ring opening of naphthalene on bulk and supported Mo<sub>2</sub>C catalysts. *Appl. Catal. A* **2007**, *324*, 9–19. [[CrossRef](#)]
45. Volpe, L.; Boudart, M. Compounds of molybdenum and tungsten with high specific surface area: I. Nitrides. *J. Solid State Chem.* **1985**, *59*, 332–347. [[CrossRef](#)]
46. Volpe, L.; Boudart, M. Compounds of molybdenum and tungsten with high specific surface area: II. Carbides. *J. Solid State Chem.* **1985**, *59*, 348–356. [[CrossRef](#)]
47. Miga, K.; Stańczyk, K.; Sayag, C.; Brodzki, D.; Djéga-Mariadassou, G. Bifunctional behavior of bulk MoO<sub>x</sub>N<sub>y</sub> and nitrided supported NiMo catalyst in hydrodenitrogenation of indole. *J. Catal.* **1999**, *183*, 63–68. [[CrossRef](#)]
48. Georginia, C.; Laredo, S.; De los Reyes, H.J.A.; Luis Cano, D.J.; Jesús Castillo, M.J. Inhibition effects of nitrogen compounds on the hydrodesulfurization of dibenzothiophene. *Appl. Catal. A* **2001**, *207*, 103–112.
49. Topsøe, H.; Clausen, B.S.; Massoth, F.E. *Hydrotreating Catalysis Science and Technology*; Springer: New York, NY, USA, 1996.
50. Abe, H.; Bell, A.T. Catalytic hydrotreating of indole, benzothiophene, and benzofuran over Mo<sub>2</sub>N. *Catal. Lett.* **1993**, *18*, 1–8. [[CrossRef](#)]
51. Nagai, M.; Miyao, T.; Tuboi, T. Hydrodesulfurization of dibenzothiophene on alumina-supported molybdenum nitride. *Catal. Lett.* **1993**, *18*, 9–14. [[CrossRef](#)]
52. Senzi, L.; Lee, J.S. Molybdenum nitride and carbide prepared from heteropolyacid: II. Hydrodenitrogenation of indole. *J. Catal.* **1998**, *173*, 134–144. [[CrossRef](#)]
53. Bunch, A.; Zhang, L.; Karakas, G.; Ozkan, U.S. Reaction network of indole hydrodenitrogenation over NiMoS/γ-Al<sub>2</sub>O<sub>3</sub> catalysts. *Appl. Catal. A* **2000**, *190*, 51–60. [[CrossRef](#)]
54. Ozkan, U.S.; Zhang, L.; Clark, P.A. Performance and postreaction characterization of γ-Mo<sub>2</sub>N catalysts in simultaneous hydrodesulfurization and hydrodenitrogenation reactions. *J. Catal.* **1997**, *172*, 294–306. [[CrossRef](#)]
55. Sayag, C.; Suppan, S.; Trawczyński, J.; Djéga-Mariadassou, G. Effect of support activation on the kinetics of indole hydrodenitrogenation over mesoporous carbon black composites-supported molybdenum carbide. *Fuel Proc. Technol.* **2002**, *77–78*, 261–267. [[CrossRef](#)]
56. Adamski, G.; Dyrek, K.; Kotarba, A.; Sojka, Z.; Sayag, C.; Djéga-Mariadassou, G. Kinetic model of indole HDN over molybdenum carbide: Influence of potassium on early and late denitrogenation pathways. *Catal. Today* **2004**, *90*, 115–119. [[CrossRef](#)]
57. Sayag, C.; Benkhaleda, M.; Suppan, S.; Trawczyński, J.; Djéga-Mariadassou, G. Comparative kinetic study of the hydrodenitrogenation of indole over activated carbon black composites (CBC) supported molybdenum carbides. *Appl. Catal. A* **2004**, *275*, 15–24. [[CrossRef](#)]
58. Ledesma, B.C.; Anunziata, O.A.; Beltramone, A.R. HDN of indole over Ir-modified Ti-SBA-15. *Appl. Catal. B* **2016**, *192*, 220–233. [[CrossRef](#)]
59. Ledesma, B.C.; Juárez, J.M.; Valles, V.A.; Anunziata, O.A.; Beltramone, A.R. Novel preparation of titania-modified CMK-3 nanostructured material as support for Ir catalyst applied in hydrodenitrogenation of indole. *Catal Lett.* **2017**, *147*, 1029–1103. [[CrossRef](#)]
60. Choi, J.-S.; Bugli, G.; Djéga-Mariadassou, G. Influence of the degree of carburization on the density of sites and hydrogenating activity of molybdenum carbides. *J. Catal.* **2000**, *193*, 238–247. [[CrossRef](#)]
61. Schlatter, J.C.; Oyama, S.T.; Metcalfe III, J.E.; Lambert, J.M., Jr. Catalytic behavior of selected transition metal carbides, nitrides, and borides in the hydrodenitrogenation of quinoline. *Ind. Eng. Chem. Res.* **1988**, *27*, 1648–1653. [[CrossRef](#)]
62. Sajkowski, D.J.; Oyama, S.T. Catalytic hydrotreating by molybdenum carbide and nitride: Unsupported Mo<sub>2</sub>N and Mo<sub>2</sub>CAI<sub>2</sub>O<sub>3</sub>. *Appl. Catal. A* **1996**, *134*, 339–349. [[CrossRef](#)]
63. Prins, R. Catalytic hydrodenitrogenation. *Adv. Catal.* **2001**, *46*, 399–464.
64. Da Costa, P.; Potvin, C.; Manoli, J.-M.; Lemberon, J.L.; Pérot, G.; Djéga-Mariadassou, G. New catalysts for deep hydrotreatment of diesel fuel: Kinetics of 4,6-dimethyldibenzothiophene hydrodesulfurization over alumina-supported molybdenum carbide. *J. Mol. Catal. A Chem.* **2002**, *184*, 323–333. [[CrossRef](#)]
65. Rota, F.; Prins, R. Mechanism of the hydrodenitrogenation of *o*-toluidine and methylcyclohexylamine over NiMo/γ-Al<sub>2</sub>O<sub>3</sub>. *Top. Catal.* **2000**, *11/12*, 327–333. [[CrossRef](#)]
66. Callant, M.; Holder, K.A.; Grange, P.; Delmon, B. Effect of the H<sub>2</sub>S and H<sub>2</sub> partial pressure on the hydrodenitrogenation (HDN) of aniline and indole over a NiMoP-γ-Al<sub>2</sub>O<sub>3</sub> catalyst. *Bull. Soc. Chim. Belg.* **1995**, *104*, 245–251. [[CrossRef](#)]

67. Laredo, G.C.; Altamirano, E.; De los Reyes, J.A. Self-inhibition observed during indole and *o*-ethylaniline hydrogenation in the presence of dibenzothiophene. *Appl. Catal. A* **2003**, *242*, 311–320. [[CrossRef](#)]
68. Piskorz, W.; Adamski, G.; Kotarba, A.; Sojka, Z.; Sayag, C.; Djéga-Mariadassou, G. Hydrodenitrogenation of indole over Mo<sub>2</sub>C catalyst: Insights into mechanistic events through DFT modeling. *Catal. Today* **2007**, *119*, 39–43. [[CrossRef](#)]
69. Mordenti, D.; Brodzki, D.; Djéga-Mariadassou, G. New synthesis of Mo<sub>2</sub>C 14 nm in average size supported on a high specific surface area carbon material. *J. Solid State Chem.* **1998**, *141*, 114–120. [[CrossRef](#)]
70. Sayag, C. Reactivite de l'oxynitruure de Molybdene dans l'hydrodeazotation de la 1,2,3,4-tetrahydroquinoleine: Adaptation de la Composition Chimique Superficielle du Solide a Celle du Melange Reactionnel. Ph.D. Thesis, University of Pierre and Marie Curie, Paris, France, 1993.
71. Mamède, A.S.; Giraudon, J.-M.; Löfberg, A.; Leclercq, L.; Leclercq, G. Hydrogenation of toluene over β-Mo<sub>2</sub>C in the presence of thiophene. *Appl. Catal. A* **2002**, *227*, 73–82. [[CrossRef](#)]
72. Xiang, C.; Chai, Y.-M.; Liu, Y.-Q.; Liu, C.-G. Mutual influences of hydrodesulfurization of dibenzothiophene and hydrodenitrogenation of indole over NiMoS/γ-Al<sub>2</sub>O<sub>3</sub> catalyst. *J. Fuel Chem. Technol.* **2008**, *36*, 684–690. [[CrossRef](#)]
73. Kim, S.C.; Massoth, F.E. Kinetics of the hydrodenitrogenation of indole. *Ind. Eng. Chem. Res.* **2000**, *39*, 1705–1712. [[CrossRef](#)]
74. Hynaux, A. Synthèse et Caractérisation de Carbures de Molybdène Supportés sur Composite de noir de Carbone Mésoporeux: Application en Hydrodésulfuration du Dibenothiophène et en Hydrodésazotation de l'indole. Ph.D. Thesis, University of Pierre and Marie Curie, Paris, France, 2006.
75. Mordenti, D. Nouvelle Methode de Preparation des Carbures de Molybdene et de Tungstene Supportes sur Charbon Actif et Reactivite en Hydrodesazotation de l'indole. Ph.D. Thesis, University of Pierre and Marie Curie, Paris, France, 1998.

**Publisher's Note:** MDPI stays neutral with regard to jurisdictional claims in published maps and institutional affiliations.



© 2020 by the authors. Licensee MDPI, Basel, Switzerland. This article is an open access article distributed under the terms and conditions of the Creative Commons Attribution (CC BY) license (<http://creativecommons.org/licenses/by/4.0/>).